Preliminary characterization of two atypical soluble guanylyl cyclases in the central and peripheral nervous system of *Drosophila melanogaster*

Kristofor K. Langlais, Judith A. Stewart and David B. Morton*

Departments of Integrative Biosciences and Cell and Developmental Biology, Oregon Health Sciences University, Portland, OR 97239, USA

*Author for correspondence (e-mail: mortonda@ohsu.edu)

Summary

Conventional soluble guanylyl cyclases form α/β heterodimers that are activated by nitric oxide (NO). Recently, atypical members of the soluble guanylyl cyclase family have been described that include the rat $\beta2$ subunit and MsGC-$\beta3$ from *Manduca sexta*. Predictions from the *Drosophila melanogaster* genome identify three atypical guanylyl cyclase subunits: *Gyc-88E* (formerly *CG4154*), *Gyc-89Da* (formerly *CG14885*) and *Gyc-89Db* (formerly *CG14886*). Preliminary data showed that transient expression of *Gyc-88E* in heterologous cells generated enzyme activity in the absence of additional subunits that was slightly stimulated by the NO donor sodium nitroprusside (SNP) but not the NO donor DEA-NONOate or the NO-independent activator YC-1. Gyc-89Db was inactive when expressed alone but when co-expressed with Gyc-88E enhanced the basal and SNP-stimulated activity of Gyc-88E, suggesting that they may form heterodimers *in vivo*. Here, we describe the localization of *Gyc-88E* and *Gyc-89Db* and show that they are expressed in the embryonic and larval central nervous systems and are co-localized in several peripheral neurons that innervate trachea, basiconical sensilla and the sensory cones in the posterior segments of the embryo. We also show that there are two splice variants of *Gyc-88E* that differ by seven amino acids, although no differences in biochemical properties could be determined. We have also extended our analysis of the NO activation of Gyc-88E and Gyc-89Db, showing that several structurally unrelated NO donors activate Gyc-88E when expressed alone or when co-expressed with Gyc-89Db.

Key words: cGMP, guanylyl cyclase, nitric oxide, *Drosophila melanogaster*, peripheral nervous system, central nervous system, NO-insensitive, sensilla, chemosensory.

Introduction

The intracellular messenger guanosine 3′5′ cyclic monophosphate (cGMP) mediates a wide variety of physiological and developmental events in many invertebrate and vertebrate species (Lucas et al., 2000; Morton and Hudson, 2002). It is the primary signaling molecule in visual transduction in vertebrates and is a regulator of vascular smooth muscle and kidney function (Lucas et al., 2000). cGMP also plays a role in several types of neuronal plasticity and in the development of the nervous system (Lucas et al., 2000; Morton and Hudson, 2002).

Guanylyl cyclases, the enzymes that catalyze the synthesis of cGMP, generally fall into one of two classes: the integral membrane receptor guanylyl cyclases and the cytoplasmic soluble guanylyl cyclases (Lucas et al., 2000). Soluble guanylyl cyclases are classically obligate heterodimers composed of an α subunit and a β subunit. The α/β heterodimers are potently activated by the gaseous messenger nitric oxide (NO) *via* a prosthetic heme group that binds to the heterodimer in the N-terminal regulatory domain (Lucas et al., 2000). Receptor guanylyl cyclases, by contrast, are homodimeric proteins that

are activated by extracellular ligands or intracellular calcium binding proteins (Lucas et al., 2000).

Recent reports have described a number of soluble guanylyl cyclases that exhibit significantly different properties compared with the conventional α/β heterodimers (Morton, 2004). One of these, MsGC-$\beta3$, was identified in the insect *Manduca sexta* (Nighorn et al., 1999). Expression of MsGC-$\beta3$ in COS-7 cells yielded moderate levels of guanylyl cyclase activity in the absence of additional subunits and this activity was not stimulated by NO donors (Nighorn et al., 1999). Gel filtration data demonstrated that MsGC-$\beta3$ formed homodimers (Morton and Anderson, 2003). Another atypical soluble guanylyl cyclase is the rat $\beta2$ subunit, which is also active in the absence of other subunits, although this activity is slightly sensitive to NO stimulation (Koglin et al., 2001).

Orthologues of MsGC-$\beta3$ have been identified in searches of the genomes of *Caenorhabditis elegans* and *Drosophila melanogaster* (Morton, 2004). The *C. elegans* MsGC-$\beta3$ orthologue, GCY-31, and the other six soluble guanylyl cyclases from *C. elegans* have all been predicted to be NO

insensitive (Morton et al., 1999). In addition to the previously studied conventional α and β subunits, the *Drosophila* genome contains three additional soluble cyclase subunits that have all been predicted to be insensitive to NO (Morton and Hudson, 2002; Morton, 2004). One of these, CG4154, is over 80% identical to MsGC-β3 and is predicted to form active homodimers (Morton and Hudson, 2002). The other two, CG14885 and CG14886, have been predicted to require an additional subunit for activity, potentially forming active heterodimers with either CG4154 or the conventional α subunit, Gycα-99B (Morton and Hudson, 2002). Rather than continue to use the CG numbers to designate these guanylyl cyclases, we propose the following designations based on their chromosomal locations: *Gyc-88E* for *CG4154*, *Gyc-89Da* for *CG14885* and *Gyc-89Db* for *CG14886*. This nomenclature is also consistent with the names of the *Drosophila* NO-sensitive subunits, *Gycα-99B* and *Gycβ-100B*. Preliminary results (Morton, 2004) confirmed that Gyc-88E yielded basal activity when expressed alone and Gyc-89Db was inactive when expressed alone. Furthermore, these studies showed that Gyc-89Db could form an active enzyme when co-expressed with Gyc-88E, although it was not tested with Gycα-99B (Morton, 2004). These studies also highlighted an unusual property of Gyc-88E; when expressed either alone or co-expressed with Gyc-89Db, it was slightly activated by the NO donor sodium nitroprusside (SNP) but not by DEA-NONOate or the NO-independent soluble guanylyl cyclase activator YC-1. These findings suggested that it was not NO itself that activated Gyc-88E but rather an additional breakdown product of SNP. The present study expands on these preliminary findings with further biochemical studies that strongly suggest that NO does indeed activate Gyc-88E and Gyc-89Db and shows that both are expressed in the central nervous system (CNS) and co-expressed in a subset of peripheral putative chemosensory neurons.

Materials and methods

Animals

Drosophila melanogaster Meigen stocks (Canton-S) were propagated in fly jars using standard procedures (Sullivan et al., 2000) at 25°C.

RNA collection

Animals were staged according to the method described by Campos-Ortega and Hartenstein (1997). Animals of selected stages were frozen and pulverized in liquid nitrogen in a pestle and mortar. Total RNA was isolated from the resulting powder with Trizol® reagent (Invitrogen, Carlsbad, CA, USA) according to the manufacturer's instructions. Poly(A)$^+$ RNA was isolated from total RNA using oligo(dT) cellulose (Ambion, Austin, TX, USA) according to the supplied protocol.

RT-PCR cloning of Gyc-88E and splice variant analysis

Superscript II RNase H reverse transcriptase (Invitrogen)

was used in a reverse transcription (RT) reaction using an oligo(dT)$_{12–18}$ primer (Invitrogen) to synthesize cDNA that was used in subsequent PCR reactions. The composition of the reaction mixture was: 50 mmol l^{-1} Tris-HCl (pH 8.3), 75 mmol l^{-1} KCl, 5 mmol l^{-1} MgCl$_2$, 10 mmol l^{-1} dithiothreitol (DTT), 0.5 μg total RNA (from a mix of larval and pupal animals), 1 μl oligo(dT)$_{12–18}$ primer (500 μg ml^{-1}), 1 μl dNTP mix (10 mmol l^{-1} each) in a total volume of 20 μl. The RT reaction was carried out at 50°C for 50 min, followed by a 15-min inactivation step at 70°C. Three primers were designed using the *Drosophila* genomic sequence located at FlyBase (accession numbers: AE003707, AE002708 and AE014297) and were used in two semi-nested PCR reactions to clone the entire open reading frame (outer primer set – 5′-CAATGTCAGCCAAGTGAAG-3′, 5′-TACATATACCCTC-TCATTAGC-3′; inner primer set – 5′-GAGGAAGT-GGATCCATG-3′, 5′-TACATATACCCTCTCATTAGC-3′) in two rounds of PCR using the Expand High Fidelity PCR System (Boehringer Mannheim, Indianapolis, IN, USA), consisting of 30 cycles with an annealing temperature of 51°C for 25 s. A 0.5 μl aliquot of the PCR reaction was used as template for subsequent amplification with the inner primers. The resulting 3 kb product was cloned into the TOPO II vector (Invitrogen). Sequencing of multiple clones revealed the existence of two splice variants (*Gyc-88E-L* and *Gyc-88E-S*) that differed by 21 bp, depending on how the 10th and 11th exons are spliced together. To determine if the splice variants were expressed in other stages, RT reactions were performed as described above on total RNA prepared from mixed larval stages or adults. Two nested sets of primers that were designed to amplify across the junction between the 10th and 11th exons were used in two rounds of PCR to produce a 70 bp or 91 bp band corresponding to *Gyc-88E-S* or *Gyc-88E-L*, respectively. The outer set of primers were 5′-GCACCAGCCAGAG-AAACG-3′ and 5′-TACATATACCCTCTCATTAGC-3′; the inner set of primers were 5′-GCAGTGCATCATTGGATC-3′ and 5′-GCAGTTGGAGTGGTTGCA-3′. The composition of the reaction mixture was: 20 mmol l^{-1} Tris-HCl (pH 8.4), 50 mmol l^{-1} KCl, 1.5 mmol l^{-1} MgCl$_2$, 200 μmol l^{-1} each dNTP, 500 nmoles of each primer, 0.5 μl reverse transcription reaction and 2.5 units of Taq DNA polymerase (Invitrogen) in a 50 μl reaction for 30 cycles with an annealing temperature of 51°C for 25 s. A 0.5 μl aliquot of the PCR reaction was used as the template for subsequent amplification, with the inner primers using the same reaction conditions. A 3% NewSieve GQA agarose gel (ISC BioExpress, Kaysville, UT, USA) was used to distinguish the two PCR products.

Northern blots

Poly(A)$^+$-selected RNA (1.5 μg) from selected stages was separated on a 1% denaturing formaldehyde agarose gel as previously described (Sambrook et al., 1989) and transferred to a Nytran SuperCharge nylon membrane using a Turboblotter (Schleicher and Schuell BioScience, Keene, NH, USA). A digoxygenin (DIG)-labeled RNA probe was generated using full-length *Gyc-88E* or a portion of the ribosomal protein RP49

(used for a loading control) with the Megascript Kit (Ambion) using DIG-UTP (Roche, Indianapolis, IN, USA). The resulting probe was hybridized to the membrane-bound transcript at 68°C using UltraHyb (Ambion), with a final probe concentration of 0.1 µmol l^{-1}. Hybridized membranes were washed for 2×10 min with low-stringency wash (2×SSC buffer, 0.1% SDS) and for 2×15 min with high-stringency wash (0.1×SSC, 0.1% SDS) at 68°C. Membranes were then incubated with Fab fragments of sheep anti-DIG-AP (alkaline phosphatase) antibody (Roche) at 1:1000 dilution in maleic acid buffer (Roche) for 1 h, followed by two 15-min washes with wash buffer (Roche). AP was detected by applying CDP-Star chemiluminescent substrate (Roche) to the membrane.

Transient expression of Gyc-88E *and* Gyc-89Db *and guanylyl cyclase assay*

To examine the enzyme activities of Gyc-88E, the full open reading frame (ORF) of *Gyc-88E-L* and *Gyc-88E-S* were subcloned into the mammalian expression vector pcDNA3.1 (Invitrogen) utilizing *Apa*I and *Kpn*I restriction enzyme sites. A cDNA of *Gyc-89Db* that contained the full ORF was obtained as an expressed sequence tag (EST) cDNA (clone ID: GH09958) from the Berkeley *Drosophila* Genome Project and subcloned into pcDNA3.1 utilizing *Eco*RI restriction enzyme sites. COS-7 cells were transiently transfected with constructs and the homogenates assayed for guanylyl cyclase activity as described previously (Morton and Anderson, 2003). 1H-[1,2,4]oxadiazole[4,3-a]quinoxalin-1-one (ODQ) was dissolved in dimethyl sulfoxide (DMSO; Sigma, St Louis. MO, USA) prior to use in guanylyl cyclase assays and was used at a final concentration of 100 µmol l^{-1}. NO donors were dissolved in distilled water or DMSO just prior to use in guanylyl cyclase assays. Sodium nitroprusside (SNP; Sigma), 3-morpholinosydnonimine (SIN-1; Calbiochem, San Diego, CA, USA), 5-[1-(phenylmethyl)-1H-indazol-3-yl]-2-furanmethanol (YC-1; Calbiochem), *S*-nitroso-*N*-acetyl-penicillamine (SNAP; Calbiochem), *S*-nitrosoglutathione (SNOG; Calbiochem), 2-(*N,N*-diethylamino)-diazenolate-2-oxide (DEA-NONOate; Calbiochem), 1-hydroxy-2-oxo-3-(*N*-ethyl-2-aminoethyl)-3-ethyl-1-triazene (NOC-12; Calbiochem) and (Z)-1-{*N*-(3-ammoniopropyl)-*N*-[4-(3-aminopropylammonio) butyl]-amino}diazen-1-ium-1,2-diolate (spermine NONOate; Calbiochem) were used at a final concentration of 100 µmol l^{-1}.

Whole-mount in situ *hybridization of embryos and larval CNS*

Whole mount *in situ* hybridization was used to identify the spatial expression pattern of *Gyc-88E* and *Gyc-89Db* during embryogenesis and in the larval CNS. DIG-labeled RNA probes were generated as described above for the northern blots and were fragmented with a carbonate buffer (60 mmol l^{-1} Na$_2$CO$_3$, 40 mmol l^{-1} NaHCO$_3$, pH 10.2) for 20 min at 65°C. Mixed stages of embryos were collected and fixed as described (Sullivan et al., 2000) and stored in 100% ethanol until use. Before use, the embryos were rehydrated with PBT (phosphate-buffered saline with 0.1% Tween 20) and

post-fixed for 30 min with 4% formaldehyde. The larval CNS was removed and fixed in 4% paraformaldehyde for 45 min, washed for 4×15 min with PBT and used the same day. Samples were prehybridized with hybridization buffer [5×SSC, 50% formamide, 0.1 mg ml^{-1} heparin sulfate, 0.1 µg ml^{-1} sonicated salmon sperm DNA (Invitrogen), 0.1% Tween 20, pH 5.2] for 1 h prior to adding probe at a final concentration of 1.5 ng µl^{-1} followed by overnight incubation at 60°C. Samples were washed for 4×1 h at 60°C in 5×SSC, 50% formamide followed by 4×15 min in PBT and blocked for 1 h with PBT plus 10% bovine serum albumin. Fab fragments of sheep anti-DIG-AP antibody (Roche) were incubated with samples at 1:1000 with PBT overnight at 4°C and washed for 4×15 min with PBT. DIG-labeled RNA probes were detected with NBT/BCIP one-step alkaline phosphatase substrate (Pierce, Rockford, IL, USA) and the reaction stopped with five rinses of 100% ethanol. For *in situ*/immunocytochemical double-label experiments, the neuronal marker antibody 22C10 (Developmental Studies Hybridoma Bank) was added (1:200) at the same time as the anti-DIG-AP antibody and was detected with horseradish peroxidase anti-mouse antiserum (Jackson ImmunoResearch, West Grove, PA, USA) at 1:1000 in PBT for 1 h. After 4×15 min washes with PBT, 22C10 was visualized with 0.5 mg ml^{-1} diaminobenzidene (DAB; Sigma) plus 0.003% hydrogen peroxide. DAB reactions were stopped with five consecutive washes with PBT. Anti-DIG antibody was then visualized as above. The samples were then dehydrated in ethanol, cleared in methyl salicylate and mounted in Permount (Fisher Scientific, Fairlawn, NJ, USA).

Results

Sequence analysis of Gyc-88E *and* Gyc-89Db

A preliminary sequence analysis of *Gyc-88E*, *Gyc-89Da* and *Gyc-89Db* based on the sequences from the annotated *Drosophila* genome has previously been described (Morton and Hudson, 2002). This analysis predicted that all three subunits should form NO-insensitive guanylyl cyclases. In addition, Gyc-88E was predicted to form an active enzyme in the absence of additional subunits, whereas Gyc-89Da and Gyc-89Db would require either Gycα-99B or Gyc-88E to form an active enzyme (Morton and Hudson, 2002). The predicted sequence of *Gyc-89Db* was confirmed from an EST clone and we used RT-PCR to obtain the cDNA for *Gyc-88E*. Sequencing multiple clones of *Gyc-88E* revealed two differences from the original annotated sequence. Firstly, all the sequenced clones had a longer C-terminal extension than originally predicted, and sequencing also revealed the existence of two splice variants, which occur through the use of alternative donor/acceptor sites to join exon 10 with exon 11 within the extended C-terminus (Fig. 1A). These corrections have now been incorporated into the most recent annotation of the *Drosophila* genome (version 3.1). The long splice variant, *Gyc-88E-L*, has an additional 21 bp compared with the short splice variant *Gyc-88E-S*, which translates into an additional seven amino acids. These additional residues

contain predicted phosphorylation sites for cGMP-dependent protein kinase (KKIT) and protein kinase C (KITFS) (Fig. 1A). Gyc-88E is over 80% identical in the N-terminal and catalytic domains to MsGC-β3 (Table 1). Fig. 1B illustrates this high degree of identity between Gyc-88E and MsGC-β3. This alignment also includes Gyc-89Db, the rat β2 subunit, which displays NO-sensitive activity in the absence

of an α subunit (Koglin et al., 2001), and a predicted MsGC-β3 orthologue from the *Anopheles gambiae* genome, CP12881. While the C-terminal extensions of Gyc-88E and MsGC-β3 are of similar lengths, they bear little similarity to each other except for two highly conserved stretches of 21 and 10 amino acids that contain several consensus phosphorylation sites. The C-terminal extension of CP12881,
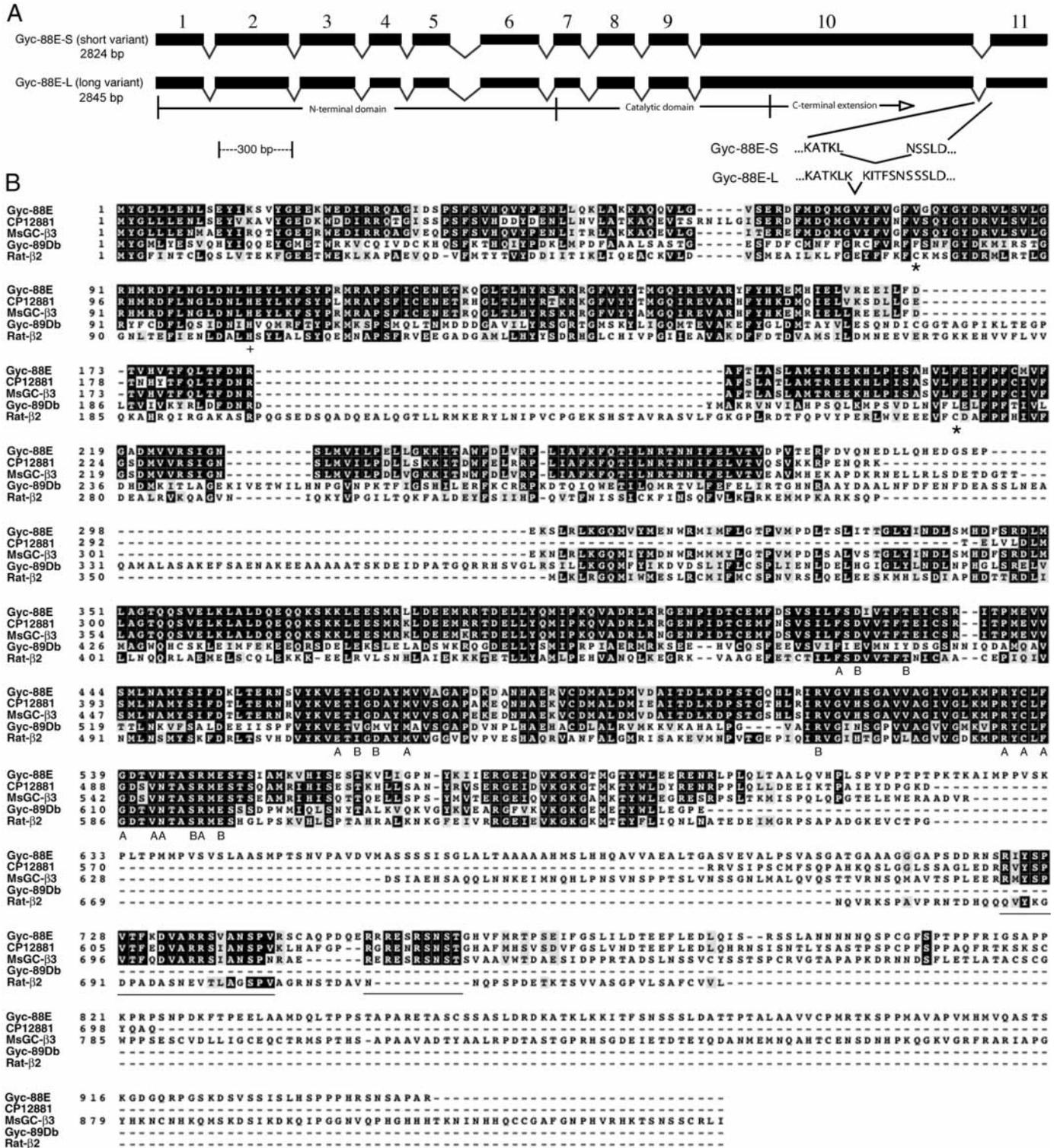

Fig. 1.

Table 1. *Comparison of the amino acid identities between Gyc-88E and selected guanylyl cyclase subunits*

	Percentage identity		
	N-terminal domain (residues 1–385)	Catalytic domain (residues 386–608)	C-terminal domain (residues 609–947)
Gyc-88E *vs* MsGC-β3	85%	81%	19%
Gyc-88E *vs* CP12881	70%	86%	18%
Gyc-88E *vs* Rat-β2	37%	49%	–
Gyc-88E *vs* Gyc-89Db	33%	43%	–
Gyc-88E *vs* Rat-β1	33%	40%	–
Gyc-88E *vs* Gycβ-100B	15%	35%	–

The sequences were aligned using ClustalW, and the percentages of residues that were identical with Gyc-88E were determined. CP12881 is the predicted orthologue of MsGC-β3 in *Anopheles gambiae* (accession number EAA01162). The positions of the functional domains are based on those of the rat β1 subunit (Namiki et al., 2001).

which is shorter than either Gyc-88E or MsGC-β3, is also poorly conserved overall but contains the two highly conserved stretches of 21 and 10 residues. Gyc-88E, Gyc-89Db and CP12881 share with MsGC-β3 the absence of two specific cysteine residues in the N-terminal domain (equivalent to cys78 and cys214 in the rat β1 subunit), which have been found to be required for NO activation in α/β heterodimers involving the rat β1 subunit (Friebe et al., 1997). The rat β2 subunit, which is slightly NO sensitive (Koglin et al., 2001), does however retain these cysteine residues. Gyc-88E and CP12881 are similar to MsGC-β3 and the rat β2

Fig. 1. Sequence analysis of *Gyc-88E* and *Gyc-89Db*. (A) Intron/exon structure and splice variants of the coding region of Gyc-88E. Exons are represented by boxes while introns are indicated with lines. The guanylyl cyclase functional domains are also indicated. The two splice variants are generated through the use of alternative splice/donor sites to vary how exons 10 and 11 are connected to yield *Gyc-88E-S* and *Gyc-88E-L*, which includes an additional 21 bp. The extra 21 bp in *Gyc-88E-L* translates into a seven amino acid stretch that contains potential PKC and PKG phosphorylation motifs, KITFS and KKIT, respectively. (B) Multiple sequence alignment of Gyc-88E and Gyc-89Db with selected atypical guanylyl cyclase subunits. The other sequences included in the alignment are MsGC-β3 (Nighorn et al., 1999), CP12881, the predicted orthologue of MsGC-β3 in *Anopheles gambiae* (accession number EAA01162), and the rat β2 subunit. Gyc-88E shares a high degree of sequence identity over the N-terminal and catalytic domains with MsGC-β3 and CP12881, whereas the C-terminal domains are more divergent, except for two highly conserved sections of 21 and 10 amino acids (underlined). Gyc-88E, MsGC-β3, CP12881 and the rat β2 subunit all have the necessary catalytic residues (marked 'B' for β subunit residues and 'A' for α subunit residues) that are predicted to be required for forming an active homodimer (see Morton and Hudson, 2002 for a more extensive discussion). By contrast, Gyc-89Db has the residues characteristic of a β subunit but is lacking some of those necessary for an α subunit. All four of the insect subunits shown lack two cysteine residues (indicated with asterisks) required for NO activation, which are present in the rat β2 subunit. A histidine residue, thought to be the axial ligand for the heme group in conventional α/β heterodimers (Zhao et al., 1998), is present in all of the subunits shown (indicated with a '+').

subunit in that they contain all of the residues predicted to interact with the Mg-GTP substrate in the homodimeric receptor guanylyl cyclases (Liu et al., 1997). This is in contrast to the classical α and β subunits, which each contain a subset of these residues, a finding that provides a rationale for the requirement of heterodimer formation with these subunits to yield an active enzyme (Liu et al., 1997). Similarly, Gyc-89Db does not contain the full complement of these residues – only containing those residues supplied by the β subunit (Fig. 1B). These analyses have predicted that Gyc-88E, like MsGC-β3 and the rat β2 subunit, will form active homodimers, whereas Gyc-89Db will require heterodimerization with either Gycα-99B or Gyc-88E to form an active enzyme (Morton and Hudson, 2002).

An unrooted phylogenetic tree generated from a ClustalX analysis illustrates the relationships between the β and β-like subunits of the soluble guanylyl cyclases (Fig. 2). MsGC-β3 clusters with its orthologues, Gyc-88E, CP12881 and the *C. elegans* gene GCY-31. Gyc-89Db clusters with Gyc-89Da, P3998 (the *Anopheles gambiae* orthologue to Gyc-89Da and Gyc-89Db) and the *C. elegans* gene GCY-33. The conventional NO-sensitive β1 subunits from vertebrates and invertebrates form a distinct cluster, while the remaining five *C. elegans* soluble guanylyl cyclase subunits and the mammalian β2 subunits form two additional separate groups.

Both Gyc-88E *splice variants are expressed in larvae and adults*

A northern blot, using *Gyc-88E* as a probe, revealed a single *Gyc-88E* transcript of approximately 6 kb (Fig. 3A). This is about twice the size of the coding region of the transcript, indicating extensive 5′ and/or 3′ untranslated regions. This transcript was present in both larval and adult stages, with apparently higher levels of transcript present in the adult (Fig. 3A).

To determine whether there was any developmental regulation of the different *Gyc-88E* splice variants, we used RT-PCR to examine their expression in larvae and adults (Fig. 3B). Two pairs of nested primers were designed to amplify a region across the splice junction to yield a 70 bp or
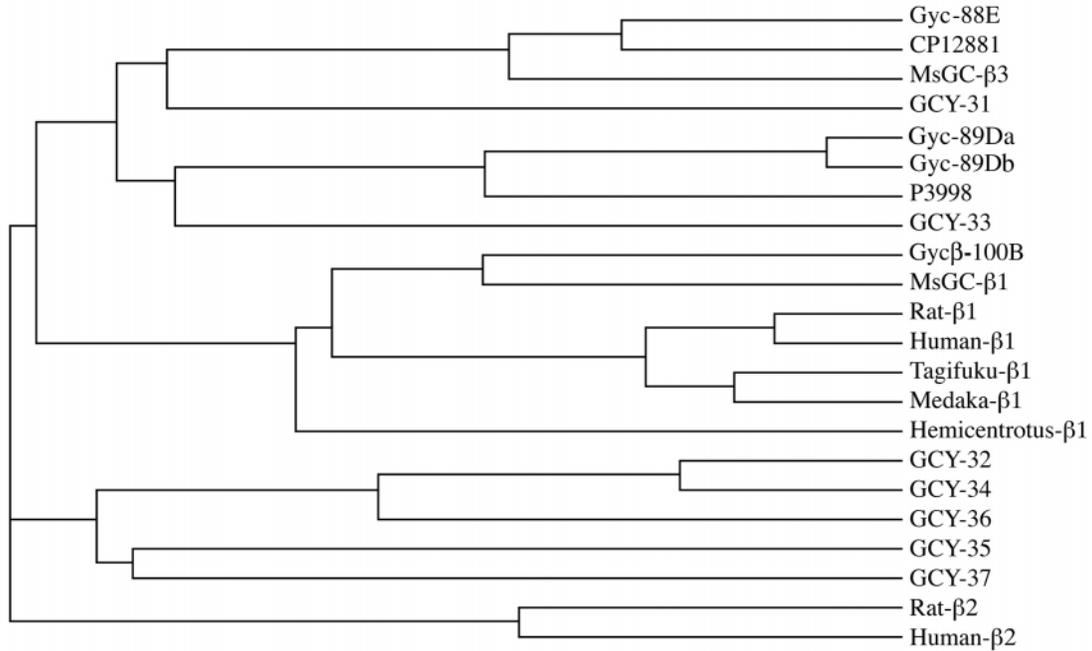
Fig. 2. Phylogenetic tree showing the relationships between the β and β-like subunits of soluble guanylyl cyclases. The first atypical guanylyl cyclase subunit characterized, MsGC-β3, clusters close to Gyc-88E, CP12881 from *Anopheles* and GCY-31 from *C. elegans*. A second grouping contains the remaining atypical subunits from *Drosophila*, Gyc-89Da, Gyc-89Db, P3998 from *Anopheles*, and GCY-33 from *C. elegans*. All the conventional soluble β1 subunits, which form NO-sensitive α1/β1 heterodimers, cluster together in a group that includes both vertebrate and invertebrate subunits. The remaining soluble guanylyl cyclases from *C. elegans* cluster together in a separate grouping and the mammalian β2 subunits also appear to form a separate distinct cluster.

91 bp product, corresponding to *Gyc-88E-S* and *Gyc-88E-L*, respectively. A high-resolution 3% agarose gel was then used to resolve the two products. We detected PCR products corresponding to both *Gyc-88E-L* and *Gyc-88E-S* in samples from both larvae and adults (Fig. 3B). The 140 bp fragment present in all lanes corresponds to genomic DNA contamination in the samples.

Guanylyl cyclase activity of Gyc-88E and Gyc-89Db

To test the predictions described above, we subcloned the *Gyc-88E* and *Gyc-89Db* open reading frames into the mammalian expression vector pcDNA3.1. These constructs were then transiently transfected in COS-7 cells and the resulting extracts assayed for guanylyl cyclase activity. As expected, and confirming previously reported preliminary data (Morton, 2004), Gyc-88E displayed basal activity in the absence of other subunits. Both splice variants of Gyc-88E were also active in the absence of additional subunits and both yielded similar levels of activity (Fig. 4A). All previously
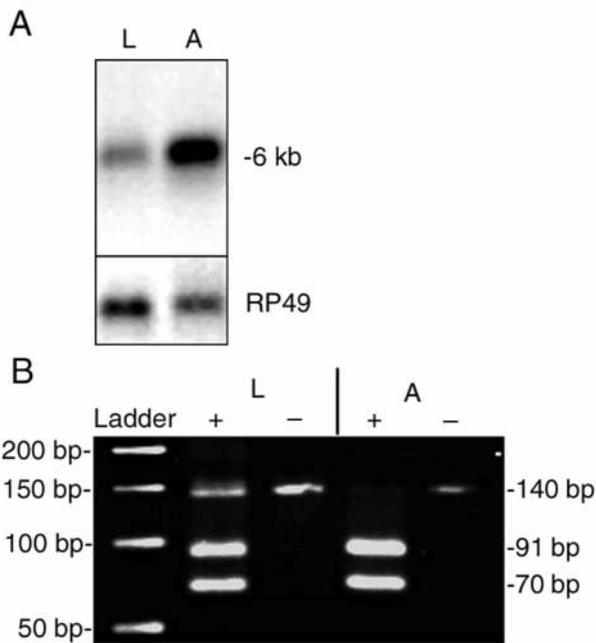

Fig. 3. Expression of *Gyc-88E* in larvae and adults. (A) Northern blot showing the 6 kb transcript for *Gyc-88E* is present in both larvae (L) and adults (A). For a loading control, membranes were stripped and re-hybridized with a DIG-labeled riboprobe for the ribosomal protein RP49. (B) Both splice variants of *Gyc-88E* are expressed in both larvae and adults. RT-PCR was used to amplify across the junction between exons 10 and 11 to distinguish between *Gyc-88E-S* and *Gyc-88E-L*. Both a 70 bp (*Gyc-88E-S*) and a 91 bp band (*Gyc-88E-L*) were detected in samples from both larvae and adults in the presence of reverse transcriptase (+). These two bands were not observed when the reverse transcriptase was omitted (–). The 140 bp band observed in all lanes results from the amplification of *Gyc-88E* genomic DNA contamination.

described guanylyl cyclases require a metal ion co-factor (Mg or Mn) for activity, with Mn yielding higher levels of activity compared with Mg (Lucas et al., 2000). Gyc-88E exhibited similar properties, with both slice variants yielding significantly higher levels of activity in the presence of Mn compared with Mg (Fig. 4A). As a comparison, we also transfected COS-7 cells with a plasmid coding for the *Manduca* guanylyl cyclase, MsGC-β3 (Nighorn et al., 1999). The activity of MsGC-β3 in the presence of either Mg or Mn was at least 10-fold higher than that of Gyc-88E (Fig. 4A), but whether this was due to an intrinsically higher level of specific activity or whether it reflected higher levels of protein expression is not known. To further investigate possible enzymatic differences between the two Gyc-88E splice variants, we assayed cell extracts for guanylyl cyclase activity in the presence of differing concentrations of GTP and either Mg or Mn (Fig. 4B). Michaelis–Menten kinetics analysis was applied to the results to examine differences in the K_m or V_{max} between the splice variants. Estimates for the value of K_m for both splice variants were similar to each other in the presence of Mg (Gyc-88E-S, 2.8±0.8 mmol l^{-1}; Gyc-88E-L, 2.5±0.6 mmol l^{-1}) and Mn (Gyc-88E-S, 0.03±0.02 mmol l^{-1}; Gyc-88E-L, 0.02±0.02 mmol l^{-1}). The values for V_{max} of the splice variants were also the same as each other in the presence of Mg (Gyc-88E-S, 6.5±0.7 pmol cGMP min^{-1} mg^{-1} protein; Gyc-88E-L, 6.0±0.6 pmol cGMP min^{-1} mg^{-1} protein) and Mn (Gyc-88E-S, 5.1±0.2 pmol cGMP min^{-1} mg^{-1} protein; Gyc-88E-L, 5.2±0.1 pmol cGMP min^{-1} mg^{-1} protein).

Previous studies showed that the NO donor SNP slightly activated Gyc-88E (Morton, 2004). Fig. 4C shows that this is also true for both of the splice variants of Gyc-88E, and again no differences are seen between the two variants. As shown previously, this increase was much smaller (2–3-fold) than seen with conventional α/β subunits such as the *Manduca* MsGC-α1/MsGC-β1 heterodimers shown here. The preliminary report on the properties of Gyc-88E showed that, although SNP was an effective activator, another NO donor (DEA-NO) was ineffective, as was YC-1 (Morton, 2004), an NO-independent activator of conventional soluble guanylyl cyclases (Friebe and Koesling, 1998). These data suggested that NO was not the active component of SNP breakdown. To further investigate this possibility, we tested whether the SNP-stimulated activity was sensitive to the conventional soluble guanylyl cyclase inhibitor ODQ. Fig. 4C shows that ODQ was ineffective at inhibiting the SNP-stimulated activity of Gyc-88E, although it was a potent inhibitor of the activation of MsGC-α1/MsGC-β1.

To examine the guanylyl cyclase activity of Gyc-89Db, we subcloned its coding sequence, obtained as an EST clone from the Berkeley *Drosophila* Genome Project (BDGP), into pcDNA3.1 and transiently expressed it into COS-7 cells. As previously demonstrated (Morton, 2004), Gyc-89Db displayed no activity when expressed in the absence of additional subunits (Fig. 4D) whether Mg or Mn was included as the metal cofactor. One possible heterodimer partner is the *Drosophila* α subunit, Gycα-99B (Morton and Hudson, 2002).

However, when we co-expressed Gycα-99B (also obtained as an EST clone from BDGP) with Gyc-89Db, we again failed to detect any enzyme activity (Fig. 4D). To test that our Gycα-99B cDNA was expressed properly, we also cloned the *Drosophila* conventional β subunit, Gycβ-100B, using RT-PCR, subcloned it into pcDNA3.1 and co-expressed it with Gycα-99B. As expected, this gave significant basal activity that was enhanced in the presence of Mn (Fig. 4D). The only other subunit that was predicted to contain the necessary residues to form an active enzyme with Gyc-89Db was Gyc-88E (Morton and Hudson, 2002). When these two subunits were co-expressed, the level of basal activity, in the presence of either Mg or Mn, was higher than when Gyc-88E was expressed alone (Fig. 4D), suggesting that Gyc-88E and Gyc-89Db are capable of forming active heterodimers and might be partners *in vivo*. No difference was seen in the levels of activity when either splice variant of Gyc-88E was co-expressed with Gyc-89Db (data not shown). As with all previously described guanylyl cyclases, the level of activity of the heterodimer was enhanced in the presence of Mn compared with Mg.

As described above, earlier studies showed that some, but not all, activators of conventional soluble guanylyl cyclases were capable of activating Gyc-88E and Gyc-88E/Gyc-89Db (Morton, 2004). To gain further insight into these differences, we tested several different classes of NO donors in guanylyl cyclase assays. We found that only SNP and the two S-nitroso compounds SNAP and SNOG were able to significantly stimulate Gyc-88E (Fig. 4E). As previously reported, DEA-NONOate was ineffective at stimulating Gyc-88E (Morton, 2004). We repeated this experiment and also tried two additional NONOates, NOC-12 and spermine NONOate, but no members of this class of NO donors were effective at stimulating Gyc-88E. In addition, again as previously reported, the NO-independent soluble guanylyl cyclase activator YC-1 was also ineffective at stimulating Gyc-88E. When Gyc-88E was co-expressed with Gyc-89Db, activity was significantly stimulated by all of the NO donors except DEA-NONOate (Fig. 4F). Not only was the basal activity of Gyc-88E enhanced when it was co-expressed with Gyc-89Db but the SNP-, SNAP- and SNOG-stimulated activity was also significantly increased. Interestingly, whereas two of the NONOates, NOC-12 and spermine NONOate, and the unrelated NO donor SIN-1 were ineffective at stimulating Gyc-88E, all three stimulated the Gyc-88E/Gyc-89Db co-expression samples. This was in contrast to DEA-NONOate, which was ineffective at stimulating Gyc-88E when expressed alone or when co-expressed with Gyc-89Db. Similarly, YC-1 was ineffective at stimulating either the Gyc-88E or the Gyc-88E/Gyc-89Db samples. By contrast, all the NO donors and YC-1 were potent activators of the *Drosophila* conventional soluble guanylyl cyclase, Gycα-99B/Gycβ-100B, and at the concentration used here (100 μmol l^{-1}) they were all similarly effective (Fig. 4G).

Gyc-88E *and* Gyc-89Db *are expressed in the peripheral and central nervous system*

To determine the cellular localization of *Gyc-88E* and
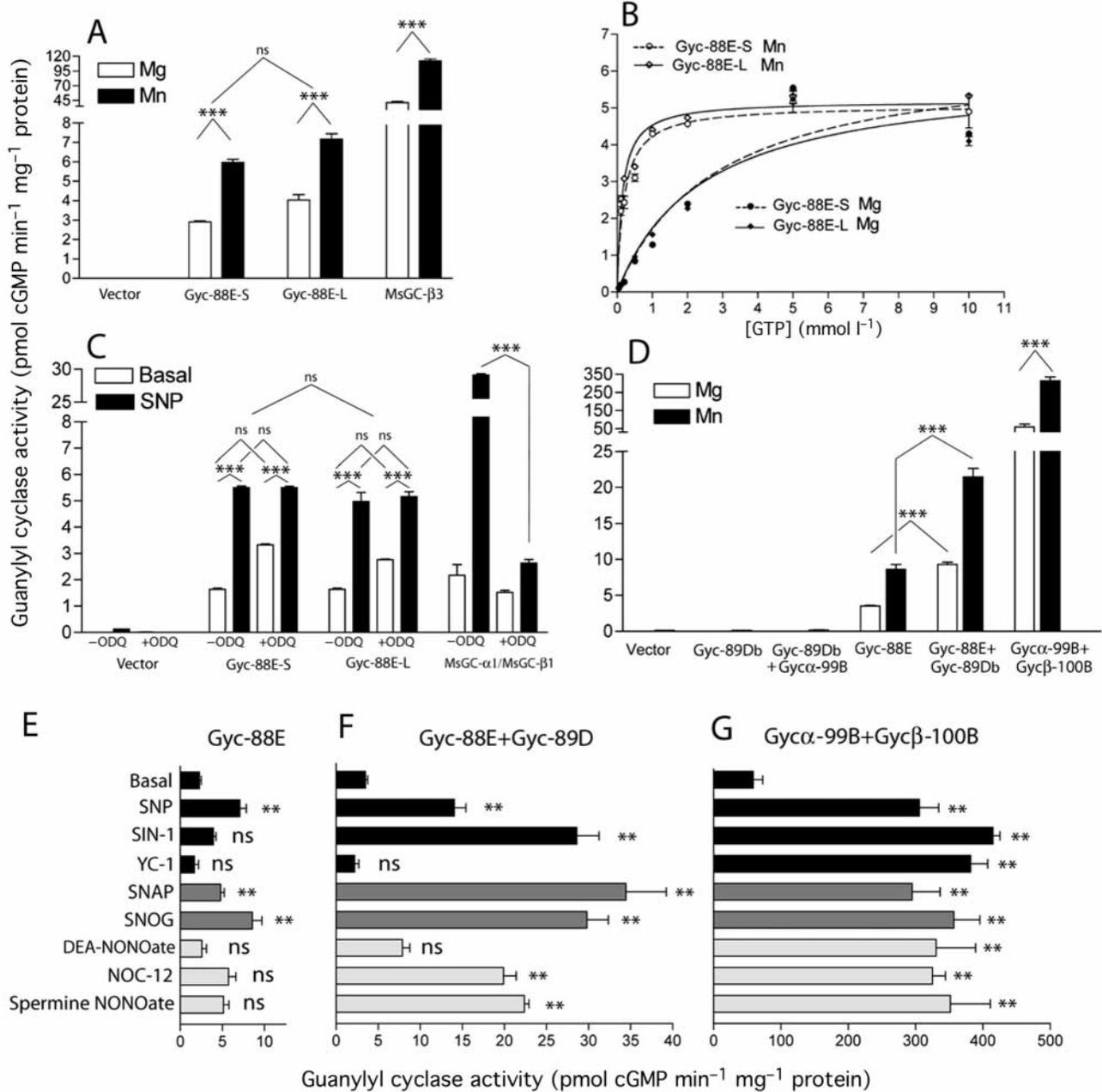
Gyc-89Db, we performed *in situ* hybridization using fragmented DIG-labeled RNA probes on whole *Drosophila* embryos and 3rd instar larval central nervous systems. *Gyc-88E* expression was detected in a segmental pattern in the ventral nerve cord (VNC) and in the brain in embryos, beginning at stage 15 or 16 and continuing through stage 17 (Fig. 5A – horizontal view; Fig. 5C – lateral view). *Gyc-89Db* showed a similar expression pattern in the VNC and brain but could be detected as early as stage 13 (data not shown) and also continued through stage 17 (Fig. 5B – horizontal view; Fig. 5D – lateral view). In stage 17 embryos, the total number of cells that expressed *Gyc-88E* was noticeably higher than the number of cells that expressed *Gyc-89Db*, especially in the brain (compare Fig. 5C and Fig. 5D). Stained single cells

visible in the anterior and posterior of the embryo in Fig. 5C,D are not part of the CNS and are discussed below. Application of a sense riboprobe generated from *Gyc-88E* or *Gyc-89Db* yielded a low level of background staining throughout the embryos with no cells stained (Fig. 5E – *Gyc-88E*; Fig. 5F – *Gyc-89Db*).

We also examined *Gyc-88E* and *Gyc-89Db* expression in the CNS of wandering 3rd instar larvae (Fig. 6). Expression of both guanylyl cyclases was observed in single cells scattered throughout the brain lobes and VNC. In the brain, expression of *Gyc-88E* and *Gyc-89Db* was most prominent in a small cluster of cells located in the anterior medial region of each lobe (Fig. 6A – *Gyc-88E*; Fig. 6B – *Gyc-89Db*). In the VNC, *Gyc-88E* and *Gyc-89Db* expression was found in both lateral

Fig. 4. Guanylyl cyclase activity of Gyc-88E and Gyc-89Db. COS-7 cells were transiently transfected with pcDNA3.1 vectors containing the open reading frames of various soluble guanylyl cyclase subunits and the cell extracts assayed for guanylyl cyclases activity under the conditions shown. (A) Gyc-88E exhibits enzyme activity in the absence of additional subunits and has higher levels of activity in the presence of Mn compared with Mg. The *Manduca* guanylyl cyclase, MsGC-β3, exhibits similar properties and was included for comparison. The two splice variants of Gyc-88E (Gyc-88E-S and Gyc-88E-L) yielded similar levels of activity as each other. Data shown are the means ± S.E.M. of three determinations. (B) Kinetic analysis of Gyc-88E-S and Gyc-88E-L. Cell extracts were assayed for guanylyl cyclase activity in the presence of $0.1–10$ mmol l^{-1} GTP in the presence of either 4 mmol l^{-1} Mg or Mn. A Michaelis–Menten curve was applied to the resulting data using Graphpad Prism 3.0. No difference in K_m or V_{max} was observed between the splice variants in the presence of Mg or Mn. (C) The NO donor sodium nitroprusside (SNP) stimulated the activity of both splice variants of Gyc-88E and this stimulation was unaffected by the guanylyl cyclase inhibitor 1H-[1,2,4]oxadiazolo[4,3,-a]quinoxaline-1-one (ODQ). By contrast, ODQ virtually eliminated the activation of the *Manduca* MsGC-α1/β1 heterodimer by SNP. Assays were carried out in the presence of 4 mmol l^{-1} Mg. Data shown are the means ± S.E.M. of three determinations. (D) Guanylyl cyclase activity of Gyc-89Db. No enzyme activity was detected when Gyc-89Db was expressed in the absence of additional subunits or when co-expressed with Gycα-99B in either the presence of 4 mmol l^{-1} Mg or 4 mmol l^{-1} Mn. However, when Gyc-89Db was co-expressed with Gyc-88E, greater basal activity was detected than when Gyc-88E was expressed alone. The basal activity was enhanced in the presence of both Mg and Mn. The data shown represent pooled values for Gyc-88E-S and Gyc-88-L, as no differences were seen between the different splice variants. Data shown represent the means ± S.E.M. of six determinations. (E–G) Guanylyl cyclase activity of the *Drosophila* soluble guanylyl cyclase subunits in the presence of 100 μmol l^{-1} of the NO donors SNP, SIN-1, SNAP, SNOG, DEA-NONOate, NOC-12 and spermine NONOate and the NO-independent activator of soluble guanylyl cyclase YC-1. The subunit combinations shown are Gyc-88E (E), Gyc-88E co-expressed with Gyc-89Db (F) and Gycα-99B/Gycβ-100B (G). The data shown represent pooled values for Gyc-88E-S and Gyc-88-L, as no differences were seen between the different splice variants. Data shown represent the means ± S.E.M. of at least four determinations. For all graphs, the data were analyzed using one-way ANOVA: 'ns' represents $P>0.05$, $**P<0.01$ and $***P<0.001$. For the data shown in A, C and D, Tukey–Kramer *post-hoc* test was used and, for E–G, Dunnett's multiple comparison test was used.

and midline cells. In the ventral region of the VNC, *Gyc-88E* (Fig. 6C) and *Gyc-89Db* (Fig. 6D) expression was found in a similar number of individual cells, with more prominent cell clusters located in the more anterior part of the VNC. In the dorsal region of the VNC, *Gyc-88E* (Fig. 6E) expression was found in a large number of cells in the lateral regions while *Gyc-89Db* (Fig. 6F) was found in noticeably fewer cells. The uniform background staining, which was most prominent in the brain lobes, was also observed in samples hybridized with sense probe (data not shown), indicating non-specific staining similar to that observed in embryo preparations (Fig. 5E,F).

In stage 17 embryos, *Gyc-88E* and *Gyc-89Db* were also expressed in a number of cells that appeared to be associated with the peripheral nervous system (Fig. 7). The overall pattern of this peripheral staining was very similar for probes to both *Gyc-88E* and *Gyc-89Db*. Both *Gyc-88E* (Fig. 7A – horizontal view; Fig. 7C – lateral view) and *Gyc-89Db* (Fig. 7B – horizontal view; Fig. 7D – lateral view) were expressed in two cells on each side of segments T1, T2 and T3 and in one cell on each side of A1 and A2. The cells in segment A2 often stained very weakly and were not always detected. The positions of the stained cells in the thoracic segments are similar to the locations of the embryonic/larval basiconical sensilla. As a preliminary test to determine whether both guanylyl cyclase subunits were co-
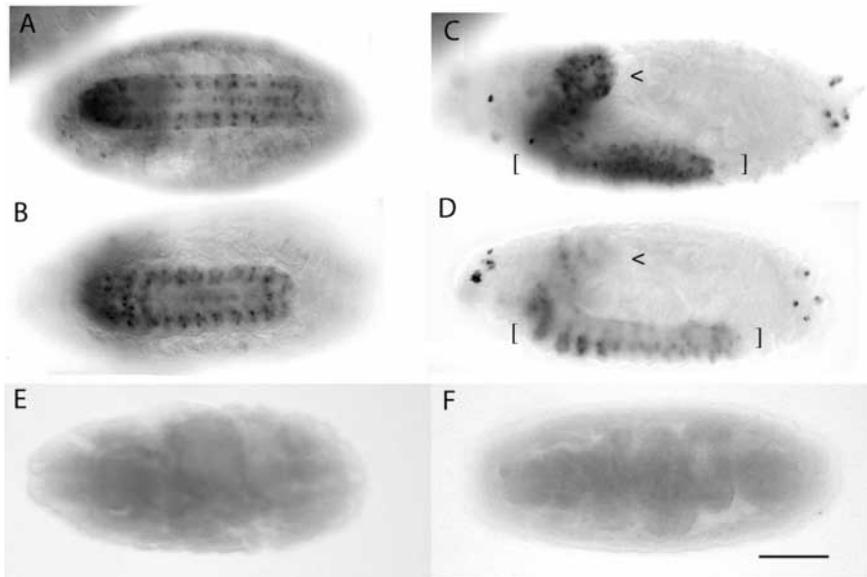

Fig. 5. Localization of *Gyc-88E* and *Gyc-89Db* expression in the central nervous system of *Drosophila* embryos. *In situ* hybridization experiments were performed on whole embryos using fragmented DIG-labeled *Gyc-88E* or *Gyc-89Db* riboprobes. (A,C) *Gyc-88E* expression in stage 16 embryos. Expression was detected in a segmental pattern in the ventral nerve cord and throughout the brain (open arrowhead). (B,D) Gyc-89Db expression in stage 17 embryos. A similar pattern of expression was detected in the ventral nerve cord and brain, although noticeably fewer cells stain in the brain with *Gyc-89Db* (open arrowhead). A and B show the horizontal view, while C and D show the lateral view. Application of a sense probe generated from *Gyc-88E* (E) or *Gyc-89Db* (F) demonstrates that the low level of ubiquitous background staining observed reflects non-specific hybridization. Anterior is always left and ventral is down in side views. Square brackets in C and D indicate the position of the ventral nerve cord. Scale bar, 100 μm.

expressed in the same cells, we hybridized embryos to both probes simultaneously. In these experiments, the number of lateral cells that stained was the same as when each probe was used individually: two cells on each side of segments T1, T2 and T3 and one cell on each side of A1 and A2 (Fig. 7E; Table 2).

In addition to the lateral cells, both probes hybridized to cells that appeared to be associated with the ganglia that innervate the head sensory organs (Fig. 7F – *Gyc-88E*; Fig. 7G – *Gyc-89Db*). *Gyc-88E* hybridized to a single pair of cells whereas *Gyc-89Db* was expressed in 2–5 closely grouped cells on each side of the embryo. In addition, the *Gyc-89Db* probe stained 4–5 closely grouped cells per side located in a more posterior position (not visible in the focal plane shown in Fig. 7G). These cells will be described in more detail later. Finally, *Gyc-88E* and *Gyc-89Db* were also found in 12 cells in segments A8 and A9 (telson; Fig. 7H – *Gyc-88E*; Fig. 7I – *Gyc-89Db*; three focal planes shown for each probe) in an apparently overlapping pattern. These cells appear to be
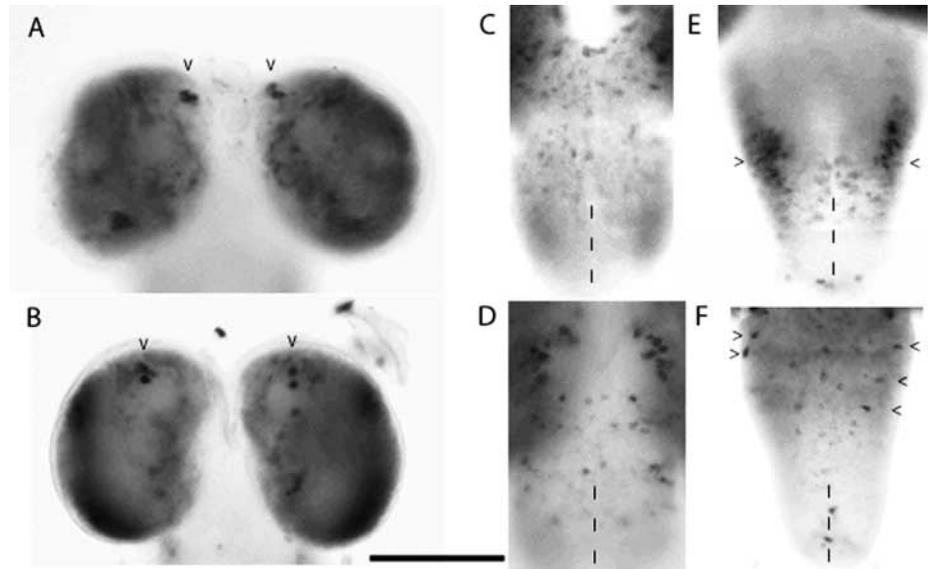

Fig. 6. *Gyc-88E* and *Gyc-89Db* expression in the central nervous system of third instar larvae. *In situ* hybridization was performed on isolated third-instar central nervous systems using the same riboprobes used in the embryo experiments. (A,B) Expression in the brain lobes. *Gyc-88E* (A) and *Gyc-89Db* (B) expression was found in scattered cells throughout the brain but was most prominent in a small cluster of cells located in the anterior medial region of each brain lobe (open arrowheads). (C–F) Expression in the ventral nerve cord. *Gyc-88E* (C,E) and *Gyc-89Db* (D,F) expression was found in scattered cells located laterally and in the midline (midline marked with broken line). The pair of images shown in C and E and in D and F are from the same preparation but are viewed at different focal planes. Anterior is up in all panels. Scale bar, 200 µm.

associated with the clusters of neurons that innervate the 10 external sensory cones found in segments A8 and A9. To determine if both probes hybridized to the same cells, we examined the preparations where both *Gyc-88E* and *Gyc-89Db* probes were used simultaneously, counted the number of cells that stained and compared these results with the number of cells stained using a single probe. We counted the same number of cells (12) in segments A8 and A9 (Fig. 7J; three focal planes shown) in the double-labeled embryos as in embryos labeled with *Gyc-88E* or *Gyc-89Db* probes individually. This suggests that both guanylyl cyclases were co-expressed in the same cells in these segments. In the anterior region of the embryo, where *Gyc-89Db* labels more cells than *Gyc-88E*, we never observed more labeled cells

Table 2. *Summary of data from the riboprobe/22C10 double label and double riboprobe experiments*

| | Head segments | | T1 | T2 or T3 lateral cluster | T2 or T3 ventral cluster | A1 or A2 ventral group | A8/A9 |
	Dorsal ganglion	Terminal ganglion					
Total neurons in ganglion or cluster per hemi-segment	~20	20+	ND	11	15	8	ND
Gyc-88E	0	1	2	1	1	1	6
Gyc-89Db	4-5	2-5	2	1	1	1	6
Both probes	4-5	2-5	2	1	1	1	6
Identity	ND	ND	ND	les	ves	v'td	ND

Diagrams of the *Drosophila* peripheral nervous system by Younossi-Hartenstein and Hartenstein (1997), Bodmer and Jan (1986), Brewster and Bodmer (1995) and Stocker (1994) were used to identify the neuron cluster or ganglion location of neurons that expressed *Gyc-88E* and *Gyc-89Db* in stage 17 embryos. Numbers refer to each side of the animal and were obtained by examining at least 50 embryos that were labeled with a riboprobe for each guanylyl cyclase, either individually or used together, and the 22C10 antibody. Embryos treated with both riboprobes stained the same number of cells in the thoracic and abdominal segments, indicating that *Gyc-88E* and *Gyc-89Db* are co-expressed in the same neurons. ND, not determined.
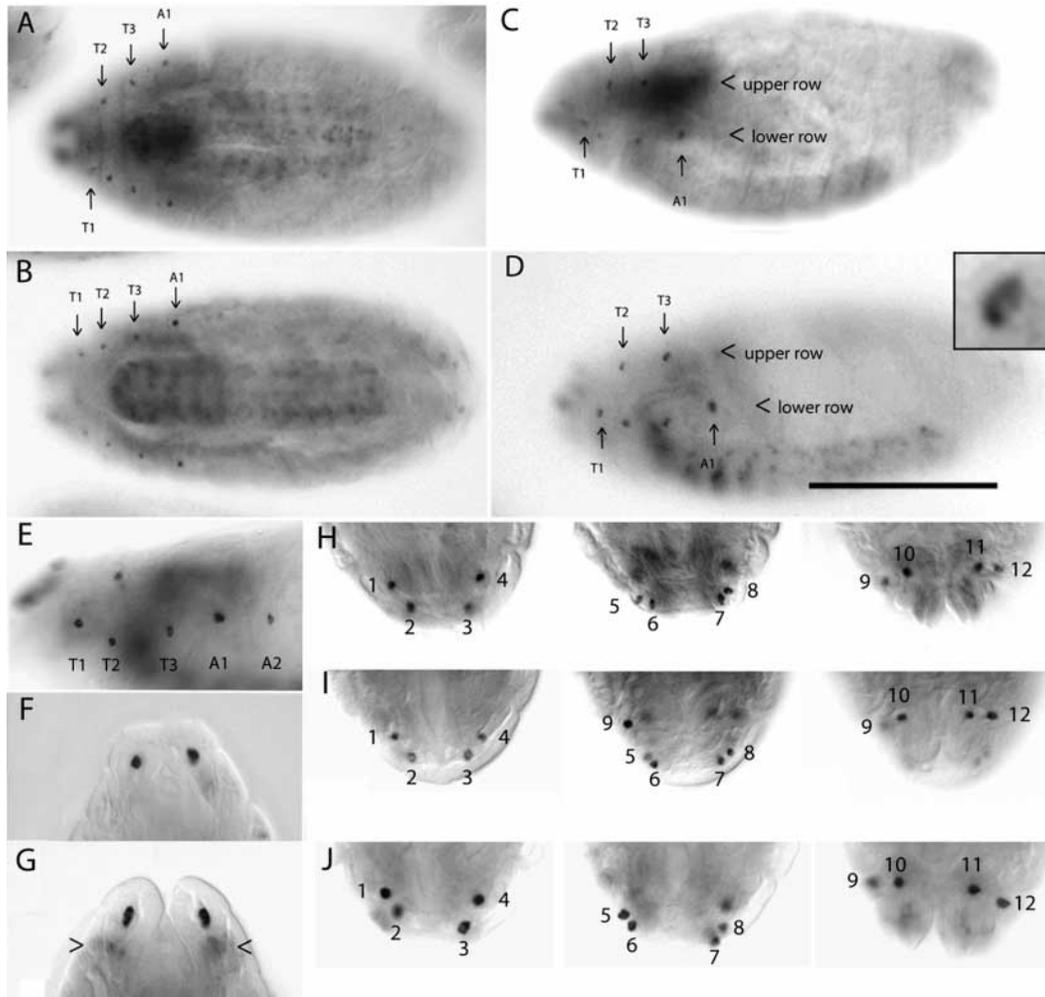
Fig. 7. Localization of *Gyc-88E* and *Gyc-89Db* in cells associated with the embryonic peripheral nervous system. *In situ* hybridization on stage 17 embryos also revealed that *Gyc-88E* or *Gyc-89Db* were both expressed in several peripherally located cells. (A,C) Expression of *Gyc-88E*. (B,D) Expression of *Gyc-89Db*. A and B show the horizontal view, while C and D show the lateral view. On each side of the embryo, two cells were detected in segments T1, T2 and T3, arranged in either an upper row or a lower row of cells, and a single cell was detected in A1 and A2. Left is always anterior and down is ventral in side views. (E) Application of both probes simultaneously resulted in the same number of cells staining in segments T1–A2 as when each probe was applied individually. (F,G) Expression of *Gyc-88E* and *Gyc-89Db* in the head segment. *Gyc-88E* (F) was expressed in a pair of cells, while *Gyc-89Db* (G) was expressed in more cells (2–5 per side in the clusters in focus, and 4–5 per side in clusters located in a more posterior position and out of focus, indicated with open arrowheads). Horizontal views are shown, and anterior is up. (H–J) Expression of *Gyc-88E* and *Gyc-89Db* in segments A8 and A9. Three consecutive focal planes of focus are shown starting from most ventral (left) to dorsal (right) to capture all cells. Both *Gyc-88E* (H) and *Gyc-89Db* (I) are expressed in a total of 12 cells. The cells are numbered arbitrarily. (J) When both probes were used simultaneously, the number of cells detected remained the same. Scale bar, 200 μm.

using both probes together than the maximum number of cells observed in the *Gyc-89Db* single probe preparations. This suggests that the cells that expressed *Gyc-88E* also expressed *Gyc-89Db*, but there were some cells that expressed only *Gyc-89Db*. These data are summarized in Table 2.

To determine if the peripheral cells that expressed *Gyc-88E* and *Gyc-89Db* in stage 17 embryos were neurons of the peripheral nervous system, we combined *in situ* hybridization with immunocytochemistry using the neuron-specific antibody 22C10 (Fig. 8). These experiments demonstrated that the *Gyc-88E*- and *Gyc-89Db*-expressing cells were always stained with 22C10 and by their positions were identified as peripheral

neurons that innervate various external sensory organs and the trachea. Comparison of our data with detailed diagrams of the peripheral nervous system (Stocker, 1994; Bodmer and Jan, 1987; Brewster and Bodmer, 1995) allowed us to more specifically identify the cell or cell cluster.

In segments T2 and T3, *Gyc-88E* and *Gyc-89Db* were co-expressed in one of the three neurons in the lateral and ventral clusters (Fig. 8A – *Gyc-88E*, lateral; Fig. 8B – *Gyc-89Db*, lateral; Fig. 8C – *Gyc-88E*, ventral; Fig. 8D – *Gyc-89Db*, ventral) that innervate the basiconical sensilla, which are external sensory organs with a putative chemosensory role (Stocker, 1994). In the lateral T2 and T3 clusters (upper row

in Fig. 7C,D), *Gyc-88E* and *Gyc-89Db* were expressed in one of the three les neurons (lateral external sensilla-innervating) (Fig. 8A – *Gyc-88E*; Fig. 8B – *Gyc-89Db*). The collected dendrites from the three les neurons were observed to project upwards to the location of the basiconical sensillum (Fig. 8A,B). In the ventral T2 and T3 clusters (lower row in Fig. 7C,D), *Gyc-88E* and *Gyc-89Db* were expressed in one of the three (ves) neurons (ventral external sensilla-innervating)
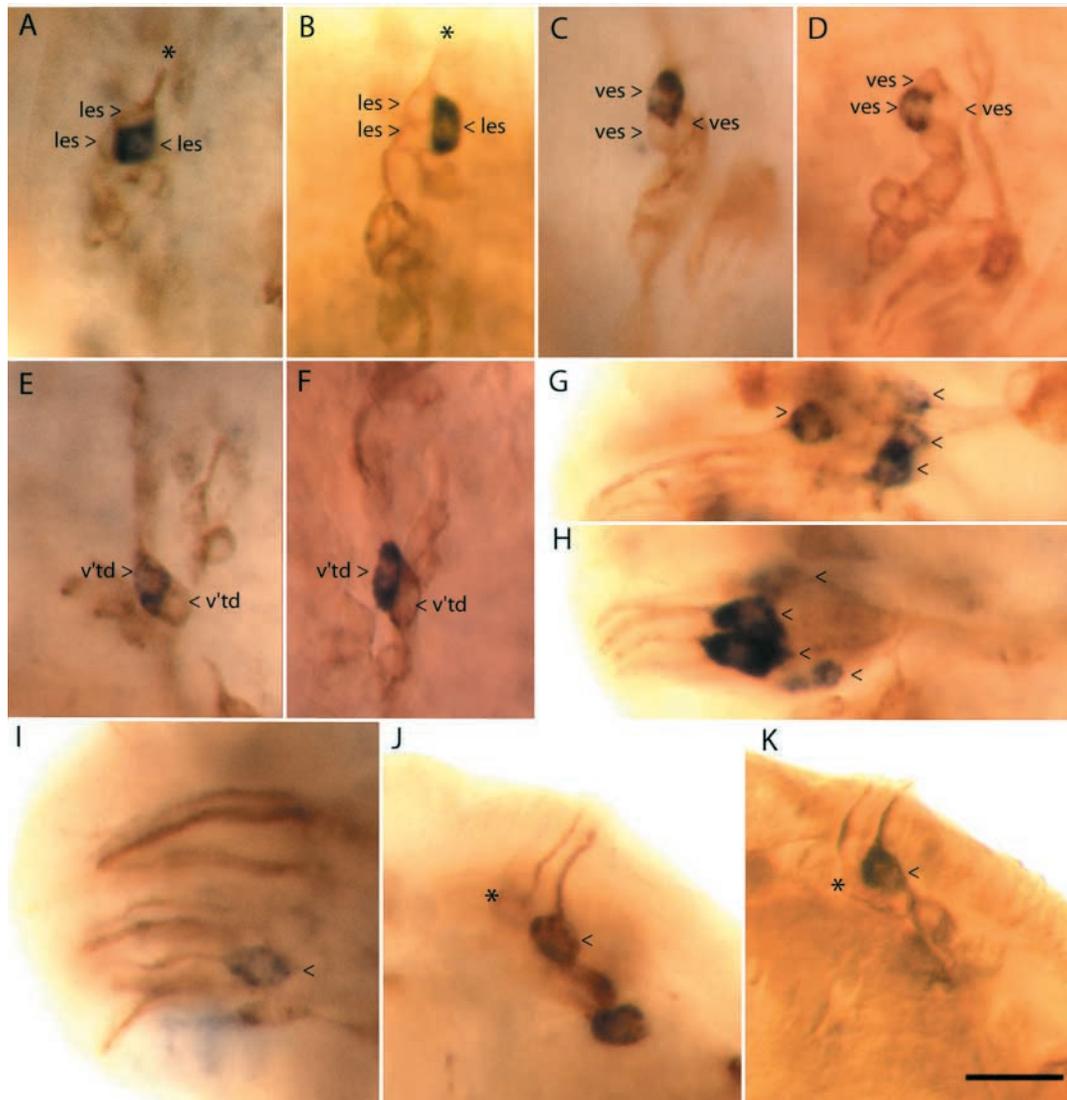

Fig. 8. *Gyc-88E* and *Gyc-89Db* are expressed in neurons of the peripheral nervous system. *In situ* hybridization (blue/black stain) was combined with immunohistochemical staining with the neuronal antibody 22C10 (brown stain). Stained cells are indicated with open arrowheads and are identified where possible. (A,B) Expression of *Gyc-88E* and *Gyc-89Db* in the lateral neuron clusters of segments T2 and T3. The example shown is segment T3 (T2 was identical). *Gyc-88E* (A) and *Gyc-89Db* (B) were expressed in one of the three les neurons that innervate a lateral external basiconical sensillum. In both of these panels, dendrites from the three les neurons can be observed to extend towards the basiconical sensillum (location marked with an asterisk). (C,D) Expression of *Gyc-88E* and *Gyc-89Db* in the ventral neuron clusters of segments T2 and T3. *Gyc-88E* (C) and *Gyc-89Db* (D) were expressed in one of the three ves neurons that innervate a ventral external basiconical sensillum. Again, the example shown is in segment T3 (T2 was identical). (E,F) Expression of *Gyc-88E* and *Gyc-89Db* in the neuron clusters of segments A1 and A2. *Gyc-88E* (E) and *Gyc-89Db* (F) were expressed in one of two v'td that innervate specific tracheal branches. The example shown is in segment A1 (A2 was identical but the staining was less intense). The stained cell was always the most anterior of the pair. (G–I) Expression of *Gyc-88E* and *Gyc-89Db* in the head segment. *Gyc-89Db* was expressed in 4–5 neurons in each of the dorsal ganglia (one on each side) (G), and in 2–5 neurons in each of the terminal (maxillary) ganglia (one on each side) (H). *Gyc-88E* expression was found in one neuron in each terminal ganglion (I). Note the dendrites projecting towards the head sensilla. (J,K) Expression of *Gyc-88E* and *Gyc-89Db* in the caudal sensory cones in the telson. *Gyc-88E* (J) and *Gyc-89Db* (K) were expressed in one of at least two neurons that innervate each of the caudal sensory cones in segment A9. The neighboring neuron that does not express guanylyl cyclase is indicated with an asterisk. In K, the dendrite is clearly seen to extend from the neuron that expressed *Gyc-89Db* to the extreme tip of the sensory cone, appearing to extend past the edge of the main body of the cone as a short protrusion. Scale bar, 30 μm.

(Fig. 8C – *Gyc-88E*; Fig. 8D – *Gyc-89Db*). In the thoracic segments, the position of the single guanylyl cyclase-expressing cell in the cluster of three external sensilla neurons was variable. In segment A1 and A2, *Gyc-88E* and *Gyc-89Db* were expressed in one of the two v'td neurons (ventral tracheal dendrite) (Fig. 8E – *Gyc-88E*; Fig. 8F – *Gyc-89Db*), which wrap their projections around specific tracheal branches (Bodmer and Jan, 1987). The stained neuron in A1 and A2 was always in the anterior-most position of the two v'td neurons.

In the anterior region of the embryo, *Gyc-89Db* was expressed in more cells than *Gyc-88E*. *Gyc-89Db* was expressed in four neurons in the dorsal ganglion (Fig. 8G). These cells correspond to the cells that were out of the plane of focus in the preparation shown in Fig. 7F. The dorsal ganglion innervates a sensory structure, known as the dorsal organ, that is thought to be the main site of olfaction in larvae (Stocker, 1994; Heimbeck et al., 1999). *Gyc-89Db* was also expressed in three large neurons and up to two more weakly stained cells in the terminal ganglion of the maxillary organ (Fig. 8H), a structure that includes several types of sensilla (Stocker, 1994). *Gyc-88E* was also expressed in the terminal ganglion but was only expressed in a single neuron (Fig. 8I). The cells of the terminal ganglion that express *Gyc-88E* and *Gyc-89Db* are the same cells that are in the focal plane in preparations shown in Fig. 7F,G.

In segments A8 and A9, *Gyc-88E* and *Gyc-89Db* were expressed in a subset of neurons that innervate the five sensory cones, which also have putative chemosensory roles (Stocker, 1994). The five sensory cones are named according to their positions – one caudal, two dorsal caudal, one dorsal lateral and one dorsal medial – and contain a combination of trichoid and basiconical sensilla (Stocker, 1994). A single neuron in each of these sensory cones was observed that expressed *Gyc-88E* and *Gyc-89Db* (Fig. 8J – *Gyc-88E*; Fig. 8K – *Gyc-89Db*). These neurons correspond to the cells numbered 2, 3 and 5–12 in Fig. 7G–I. In some cases, it was possible to trace the dendrite from the neuron that stained for *Gyc-88E* or *Gyc-89Db* to the tip of the sensory cone (Fig. 8K), a characteristic of chemosensory neurons (Dambly-Chaudiere et al., 1992). The remaining two neurons, numbered 1 and 4 in Fig. 7G–I, had dendrites that projected in a posterior direction, but we could not determine their target of innervation because it was not possible to follow them to their terminus.

Discussion
Sequence analysis of Gyc-88E *and* Gyc-89Db

This report further describes the initial characterization of two atypical soluble guanylyl cyclase subunits from *Drosophila* that we have designated *Gyc-88E* and *Gyc-89Db*. The *Drosophila* genome contains five genes that code for soluble guanylyl cyclase subunits (Morton and Hudson, 2002; Morton, 2004) and only two of these, *Gycα-99B* (*dgc-α1*) and *Gycβ-100B* (*dgc-β1*), have been characterized (Shah and Hyde, 1995; Gibbs et al., 2001). *Gycα-99B* and *Gycβ-100B* are the orthologues of the conventional mammalian α1 and β1

subunits, which form obligate α/β heterodimers that are potently activated by the gaseous messenger molecule NO (Lucas et al., 2000). One of the remaining three, *Gyc-88E*, is the orthologue of MsGC-β3, a *Manduca sexta* soluble guanylyl cyclase subunit that forms active homodimers and is insensitive to NO (Nighorn et al., 1999; Morton and Anderson, 2003). Additional orthologues of MsGC-β3 include CP12881, a predicted subunit identified in the *A. gambiae* genome, and GCY-31, identified in *C. elegans.* The remaining two *Drosophila* soluble cyclases, *Gyc-89Da* and *Gyc-89Db*, fall into a previously uncharacterized β-like subunit group that includes P3998 from *Anopheles* and GCY-33 in *C. elegans*. *Gyc-89Da* and *Gyc-89Db* are 83% identical to each other and are located adjacent to each other on the genome, suggesting the occurrence of a recent gene duplication event. As the *Anopheles* genome appears to only have a single copy of an orthologous gene, this duplication is likely to have occurred after the divergence of these two dipterans.

A structural feature that Gyc-88E shares with MsGC-β3 and CP12881 is a long C-terminal extension (Fig. 1) that is not found in β1 subunits. The C-terminal extensions of MsGC-β3, Gyc-88E and the *Anopheles* orthologue CP12881 are highly divergent, except for two conserved stretches of 21 and 10 amino acids, suggesting that these regions play an important role in enzymatic regulation. Removing the entire C-terminal extension from MsGC-β3 decreased the K_m in the presence of Mg, while no change was measured in the presence of Mn (Morton and Anderson, 2003). These results suggested that the C-terminal domain formed an auto-inhibitory domain in MsGC-β3 (Morton and Anderson, 2003). The estimated values for K_m for Gyc-88E were similar to those for MsGC-β3, in particular the almost 20-fold reduction in the presence of Mn compared with Mg, suggesting that the C-terminal domain of Gyc-88E might also be inhibitory. However, removal of this domain in Gyc-88E did not produce any change in the kinetic parameters (K.K.L. and D.B.M., unpublished data). An interesting feature with a potential role in regulation that is not found in the C-terminal extensions of MsGC-β3 or CP12881 are the phosphorylation motifs located in the seven additional residues found in the Gyc-88E-L splice variant (Fig. 1A). While no differences in the activity or kinetics were found between the splice variants in this study, it is possible that phosphorylation of this site alters Gyc-88E-L activity.

Biochemical properties of Gyc-88E and Gyc-89Db

Gyc-88E shares a number of unusual sequence and structural features with MsGC-β3. Firstly, like the receptor guanylyl cyclases and unlike all known β1 subunits, both Gyc-88E and MsGC-β3 possess all of the residues thought to interact with the Mg-GTP substrate (Fig. 1B; for a detailed discussion of homodimer/heterodimer predictions and a model of the catalytic site, see Morton and Hudson, 2002). Previous studies showed that MsGC-β3 does yield basal activity in the absence of other subunits (Nighorn et al., 1999) and forms homodimers (Morton and Anderson, 2003). These studies formed the basis for the prediction that Gyc-88E would also yield basal activity

in the absence of other subunits, a prediction demonstrated to be correct in this and a previous study (Fig. 4; Morton, 2004). While MsGC-β3 yielded higher levels of basal activity than Gyc-88E, the basal activity of Gyc-88E was nevertheless similar to that of the *Manduca* α1/β1 heterodimer. Unlike all known β1 subunits and the mammalian β2 subunits, both Gyc-88E and MsGC-β3 have substitutions at two cysteine residues known to be crucial for heme binding and NO activation in the rat β1 subunit (Friebe et al., 1997; Fig. 1B). Extracts made from COS-7 cells transiently transfected with MsGC-β3 yielded no increase in activity over basal levels when NO donors were applied (Nighorn et al., 1999). This observation, together with its sequence features, led to the prediction that Gyc-88E would also be NO-insensitive (Morton and Hudson, 2002).

Preliminary data suggested that this was in fact the case. Although SNP slightly activated Gyc-88E, another structurally unrelated NO donor, DEA-NONOate, was ineffective (Morton, 2004). Furthermore, an NO-independent activator of conventional soluble guanylyl cyclases, YC-1, was also ineffective (Morton, 2004). This suggested that the mechanism of activation of Gyc-88E was quite distinct from that of conventional α/β heterodimers and that it was likely to be another breakdown product of SNP and not NO that activated Gyc-88E. Results from the present study, however, suggest that NO might be capable of activating Gyc-88E. Although DEA-NONOate was again found to be ineffective, several other structurally unrelated NO donors yielded a small but significant increase in activity. However, compared with the 10–20-fold stimulation of conventional α/β heterodimers, stimulation of Gyc-88E was only 2–3-fold. Four different structural classes of NO donors were tested for their ability to activate Gyc-88E. SNP and two *S*-nitroso compounds (SNAP and SNOG) stimulated Gyc-88E whereas three different NONOates and an unrelated compound, SIN-1, were ineffective.

As predicted and previously reported (Morton, 2004), Gyc-89Db showed no activity when expressed alone but formed an active guanylyl cyclase when co-expressed with Gyc-88E. Here, we show that Gyc-88E and Gyc-89Db are likely to form heterodimers *in vivo*. Not only are they co-expressed in many of the same cells but no activity was detected when Gyc-89Db was co-expressed with its other predicted partner, the conventional α subunit, Gycα-99B. It is possible that Gyc-88E and Gycα-99B dimerize, as do MsGC-β3 and MsGC-α1 (Morton and Anderson, 2003), but, possibly due to misfolding, these heterodimers are inactive. In addition to increased basal activity, Gyc-88E and Gyc-89Db yielded higher levels of activity in the presence of NO donors compared with when Gyc-88E was expressed alone. As with Gyc-88E, not all NO donors were effective at stimulating the activity of the Gyc-88E/Gyc-89Db heterodimers, but some compounds (SIN-1 and two of the NONOates) that were ineffective at stimulating Gyc-88E did stimulate the heterodimer. Although DEA-NONOate failed to significantly increase the activity of the heterodimer, it did appear to have a small positive effect. YC-1 was also ineffective at stimulating the heterodimer. These results contrast with the effects on the conventional α/β

heterodimer, where all the compounds tested were effective at stimulating guanylyl cyclase activity. The fact that several different structural classes of NO donors were capable of activating both Gyc-88E and the Gyc-88E/Gyc-89Db heterodimers suggests that NO, rather than another breakdown product of these compounds, was the active component in these experiments. This conclusion was strengthened by our finding that 1 mmol l^{-1} sodium cyanide (SNP breakdown also produces cyanide ions) failed to stimulate Gyc-88E (data not shown).

It is unclear why SNP and the *S*-nitroso compounds were able to significantly stimulate Gyc-88E while other compounds failed to do so. Also unknown are why some of the NONOates were capable of stimulating the Gyc-88E/Gyc-89Db heterodimer whereas DEA-NONOate was ineffective and why none of the NONOates were capable of activating Gyc-88E. It is notable that SNAP and SNOG have a considerably longer half-life of NO release than the other NO donors used (hours rather than minutes), and DEA-NONOate has the shortest half-life of the NONOates tested. All these compounds were approximately equally effective at stimulating the conventional Gycα-99B/Gycβ-100B heterodimers at the concentrations used. If this concentration is supramaximal for the conventional subunits, but submaximal for Gyc-88E and Gyc-89Db, then the lower concentration of free NO with some of the donors could explain the data. In addition, although there was no statistically significant increase in activity of Gyc-88E in the presence of the NONOates, they all showed a slight increase. Further dose–response studies of the different donors might resolve this issue.

Our experiments with ODQ further illustrate differences between the heme group/regulatory domains of the two soluble guanylyl cyclases studied in this report and conventional α/β heterodimers. ODQ, which is known to block NO stimulation of the α/β heterodimers by oxidation of the heme group, had no inhibitory effect on the SNP stimulation of Gyc-88E. The regions of the regulatory domain in Gyc-88E and/or Gyc-89Db that are responsible for these biochemical differences remain to be discovered.

As the NO donors at most only weakly stimulate Gyc-88E and Gyc-89Db, and MsGC-β3 is insensitive to NO donors, it seems unlikely that NO is the activator of members of the β3 family *in vivo*. Although the nature of the *in vivo* activator is unknown, there are some suggestions based on studies of MsGC-β3. There is circumstantial evidence that MsGC-β3 is activated by the neuropeptide eclosion hormone *via* a pathway that might be mediated by protein kinases (see Morton and Simpson, 2002). The cells that express Gyc-88E, however, do not appear to include likely eclosion hormone target cells in *Drosophila* (Baker et al., 1999). Nevertheless, the location of potential phosphorylation sites in conserved regions of the C-terminal domain of Gyc-88E suggests that phosphorylation might be a mechanism of activation of this family of guanylyl cyclases.

Localization of Gyc-88E *and* Gyc-89D *expression*

Evidence that supports the formation of Gyc-88E and

Gyc-89Db heterodimers *in vivo* was provided by *in situ* hybridization using probes to both subunits simultaneously. In these experiments, the use of both probes did not label an increased number of cells in the peripheral nervous system compared with using a single probe. The number of cells stained in thoracic and abdominal segments was identical when either probe was used individually or when both probes were used together, suggesting that all these peripheral cells expressed both *Gyc-88E* and *Gyc-89Db* (see Table 2). In the head segment, however, the total number of cells that we detected was more variable. Nevertheless, we never observed more stained cells in the double-probe *in situ* experiments than the maximum number of cells observed when probing for *Gyc-89Db* alone (see Table 2). These experiments suggest that some of the anterior cells express both *Gyc-88E* and *Gyc-89Db* while others express only *Gyc-89Db*. Co-immunoprecipitation experiments are needed to definitively demonstrate heterodimer formation.

Although there are many cells that appear to co-express *Gyc-88E* and *Gyc-89Db*, there are several places where only one of the cyclases is expressed. In addition to the peripheral cells in the head segments, *Gyc-89Db* was expressed in the CNS at earlier stages than *Gyc-88E*. Because Gyc-89Db was only active in the guanylyl cyclase assays co-expressed with Gyc-88E, it is not clear what the function of Gyc-89Db is when expressed alone. It is possible that the *Gyc-88E* transcript was present in these cells but was present at levels too low to be detected with *in situ* experiments or that the *Gyc-89Db* transcript was present but was not translated. Alternatively, Gyc-89Db may be playing a dominant negative role, by heterodimerizing with other soluble guanylyl cyclase subunits and thus preventing them from dimerizing with subunits that would yield an active guanylyl cyclase dimer. A similar situation has been found with MsGC-β3, which will form inactive heterodimers *in vitro* with MsGC-α1 and MsGC-β1 (Morton and Anderson, 2003).

In the present study, we have primarily focused on the expression of *Gyc-88E* and *Gyc-89Db* in the embryonic peripheral nervous system, where they are co-expressed in a subset of peripheral neurons. We were able to identify several of the cells staining for both guanylyl cyclases in segments T2 and T3 as one of three neurons (les in the lateral cluster and ves in the ventral cluster) that innervate the basiconical sensilla. Basiconical sensilla are external club-like structures with pore-like openings to the outside environment and have a putative hygroreceptor or chemosensory role (Stocker, 1994; Younossi-Hartenstein and Hartenstein, 1997). We also found neurons staining for both guanylyl cyclases in segment A8 and A9 that innervate all of the posterior cone-shaped external sensilla (Campos-Ortega and Hartenstein, 1997). We could not, however, specifically name these neurons, as they are part of large clusters that have not been characterized in great detail. These sensory cones possess both trichoid and basiconical sensilla (Campos-Ortega and Hartenstein, 1997). Consistent with a role in chemoreception, we observed a neuronal cell body stained for guanylyl cyclase that extended a single dendrite to the very tip of a sensillum (Fig. 8K), a distinguishing feature of chemosensory neurons (Dambly-Chaudiere et al., 1992). In segments A1 and A2, *Gyc-88E* and *Gyc-89Db* were expressed in the anterior-most of the two v'td neurons, each of which innervates specific non-overlapping tracheal branches. The function of these neurons is not known. The double-label experiments also allowed us to determine the location of the guanylyl cyclase-expressing cells we observed in the head segment. *Gyc-88E* stained one neuron in each of the two terminal ganglia while *Gyc-89Db* stained 2–5 neurons in each of the terminal ganglia and 4–5 neurons in each of the two dorsal ganglia. The terminal ganglion innervates the maxillary organ, which is known to serve a gustatory function and has at least six different types of sensilla (Stocker, 1994; Heimbeck et al., 1999; Oppliger et al., 2000). The dorsal ganglion innervates the dorsal or antennal organ, which consists of seven different sensilla and is the main olfactory organ in larval *Drosophila* (Stocker, 1994; Heinbeck et al., 1999; Oppliger et al., 2000). It was not possible to determine which sensilla were innervated by the neurons that expressed *Gyc-88E* and *Gyc-89Db*.

Expression of *Gyc-88E* and *Gyc-89Db* in peripheral neurons that innervate various external sensilla and the trachea was also detected in newly hatched first-instar larvae (data not shown), suggesting that these guanylyl cyclases play a role in sensory transduction during larval life. Guanylyl cyclases and cGMP signaling have been demonstrated to play an important role in several types of sensory transduction in both vertebrates and invertebrates (reviewed in Kramer and Molokanova, 2001; Morton and Hudson, 2002). For example, cGMP produced by a receptor guanylyl cyclase is the primary signal molecule in vertebrate phototransduction (Kramer and Molokanova, 2001). In *Drosophila*, cGMP appears to play a modulatory role in phototransduction and olfaction, rather than being involved in the primary transduction pathway (Bacigalupo et al., 1995; Morton and Hudson, 2002). In the silkmoth (*Bombyx mori*), soluble and particulate guanylyl cyclase activity was measured in the antennae, and in *Manduca* the receptor-like guanylyl cyclase MsGC-I was detected in olfactory receptor neurons (Nighorn et al., 2001). In *C. elegans*, several different receptor guanylyl cyclases are expressed in olfactory neurons (Yu et al., 1997). Two of these, ODR-1 and DAF-11, are co-expressed in the chemosensory neuron AWC, and mutations to either gene resulted in the abolishment of chemotaxis to all AWC-sensed odorants (Birnby et al., 2001; L'Etoile and Bargmann, 2000).

Another possible role for the cGMP formed in neurons by Gyc-88E and Gyc-89Db is axonal path-finding (Schmidt et al., 2002). While *Gyc-88E* expression was detectable only in later embryonic stages when most axonal path-finding events have already occurred, *Gyc-89Db* expression was detectable in the peripheral nervous system at stages that coincide with axonal path-finding events (stage 13–16; Campos-Ortega and Hartenstein, 1997). Thus, it is possible that Gyc-89Db plays a role in both peripheral nervous system development and sensory transduction.

Both *Gyc-88E* and *Gyc-89Db* were also expressed in the embryonic and larval central nervous systems. *Gyc-89Db* expression in the CNS began as early as stage 12 (data not

shown) and continued at a constant level through embryogenesis. *Gyc-88E* expression in the CNS was first detectable at stage 15 or 16. *Gyc-88E* expression continued throughout embryogenesis but expanded to an increased number of cells throughout the CNS by the end of stage 17. Both *Gyc-88E* and *Gyc-89Db* were expressed in a number of cells in the brain and VNC of third-instar larvae. At this point it is difficult to speculate on the function of these guanylyl cyclases in the nervous system during embryonic development and in larvae, but roles for cGMP signaling have been demonstrated in axon guidance (Nishiyama et al., 2003), synapse formation (Leamey et al., 2001; Gibbs et al., 2001) and cell migration (Haase and Bicker, 2003).

The discovery of atypical soluble guanylyl cyclases that are insensitive or relatively insensitive to NO in *Drosophila*, *Manduca* and *C. elegans* suggests the existence of novel pathways upstream of soluble guanylyl cyclase that do not involve NO. The presence of atypical guanylyl cyclases in neurons of the peripheral nervous system of *Drosophila* that are amenable to physiological and genetic experimentation should provide new avenues to examine the function and regulation of these unusual enzymes.

References

Bacigalupo, J., Bautista, D. M., Brink, D. L., Hetzer, J. F. and O'Day, P. M. (1995). Cyclic-GMP enhances light-induced excitation and induces membrane currents in *Drosophila* retinal photoreceptors. *J. Neurosci.* **15**, 7196-7200.

Baker, J. D., McNabb, S. L. and Truman, J. W. (1999). The hormonal coordination of behavior and physiology at adult ecdysis in *Drosophila melanogaster*. *J. Exp. Biol.* **202**, 3037-3048.

Birnby, D. A., Link, E. M., Vowels, J. J., Tian, H., Colacurcio, P. L. and Thomas, J. H. (2000). A transmembrane guanylyl cyclase (DAF-11) and Hsp90 (DAF-21) regulate a common set of chemosensory behaviors in *Caenorhabditis elegans*. *Genetics* **155**, 85-104.

Bodmer, R. and Jan, Y. N. (1987). Morphological differentiation of embryonic peripheral neurons in *Drosophila*. *Roux's Arch. Dev. Biol.* **196**, 69-77.

Brewster, R. and Bodmer, R. (1995). Origin and specification of type II sensory neurons in *Drosophila*. *Development* **121**, 2923-2936.

Campos-Ortega, J. A. and Hartenstein, V. (1997). *The Embryonic Development of* Drosophila melanogaster. New York: Springer-Verlag.

Dambly-Chaudiere, C., Jamet, E., Burri, M., Bopp, D., Basler, K., Hafen, E., Dumont, N., Spielmann, P., Ghysen, A. and Noll, M. (1992). The paired box gene pox neuro: a determinant of poly-innervated sense organs in *Drosophila*. *Cell* **69**, 159-172.

Friebe, A. and Koesling, D. (1998). Mechanism of YC-1-induced activation of soluble guanylyl cyclase. *Mol. Pharmacol* **53**, 123-127.

Friebe, A., Wedel, B., Harteneck, C., Foerster, J., Schultz, G. and Koesling, D. (1997). Functions of conserved cysteines of soluble guanylyl cyclase. *Biochemistry* **36**, 1194-1198.

Gibbs, S. M., Becker, A., Hardy, R. W. and Truman, J. W. (2001). Soluble guanylate cyclase is required during development for visual system function in *Drosophila*. *J. Neurosci.* **21**, 7705-7714.

Haase, A. and Bicker, G. (2003). Nitric oxide and cyclic nucleotides are regulators of neuronal migration in an insect embryo. *Development* **130**, 3977-3987.

Heimbeck, G., Bugnon, V., Gendre, N., Haberlin, C. and Stocker, R. F. (1999). Smell and taste perception in *Drosophila melanogaster* larva: toxin expression studies in chemosensory neurons. *J. Neurosci.* **19**, 6599-6609.

Koglin, M., Vehse, K., Budaeus, L., Scholz, H. and Behrends, S. (2001). Nitric oxide activates the beta 2 subunit of soluble guanylyl cyclase in the absence of a second subunit. *J. Biol. Chem.* **276**, 30737-30743.

Kramer, R. H. and Molokanova, E. (2001). Modulation of cyclic-nucleotide-gated channels and regulation of vertebrate phototransduction. *J. Exp. Biol.* **204**, 2921-2931.

L'Etoile, N. D. and Bargmann, C. I. (2000). Olfaction and odor discrimination are mediated by the *C. elegans* guanylyl cyclase ODR-1. *Neuron* **25**, 575-586.

Leamey, C. A., Ho-Pao, C. L. and Sur, M. (2001). Disruption of retinogeniculate pattern formation by inhibition of soluble guanylyl cyclase. *J. Neurosci.* **21**, 3871-3880.

Liu, Y., Ruoho, A. E., Rao, V. D. and Hurley, J. H. (1997). Catalytic mechanism of the adenylyl and guanylyl cyclases: modeling and mutational analysis. *Proc. Natl. Acad. Sci. USA* **94**, 13414-13419.

Lucas, K. A., Pitari, G. M., Kazerounian, S., Ruiz-Stewart, I., Park, J., Schulz, S., Chepenik, K. P. and Waldman, S. A. (2000). Guanylyl cyclases and signaling by cyclic GMP. *Pharmacol. Rev.* **52**, 375-414.

Morton, D. B. (2004). Invertebrates yield a plethora of atypical guanylyl cyclases. *Mol. Neurobiol.* **29**, 97-116.

Morton, D. B. and Anderson, E. A. (2003). MsGC-β3 forms active homodimers and inactive heterodimers with NO-sensitive soluble guanylyl cyclase subunits. *J. Exp. Biol.* **206**, 937-947.

Morton, D. B. and Hudson, M. L. (2002). Cyclic GMP regulation and function in insects. *Adv. Insect Physiol.* **29**, 1-54.

Morton, D. B. and Simpson, P. J. (2002). Cellular signaling in eclosion hormone action. *J. Insect Physiol.* **48**, 1-13.

Morton, D. B., Hudson, M. L., Waters, E. and O'Shea, M. (1999). Soluble guanylyl cyclases in *Caenorhabditis elegans*: NO is not the answer. *Curr. Biol.* **9**, R546-R547.

Namiki, S., Hirose, K. and Iino, M. (2001). Mapping of heme-binding domains in soluble guanylyl cyclase β1 subunit. *Biochem. Biophys. Res. Commun.* **288**, 798-804.

Nighorn, A., Byrnes, K. A. and Morton, D. B. (1999). Identification and characterization of a novel beta subunit of soluble guanylyl cyclase that is active in the absence of a second subunit and is relatively insensitive to nitric oxide. *J. Biol. Chem.* **274**, 2525-2531.

Nighorn, A., Simpson, P. J. and Morton, D. B. (2001). The novel guanylyl cyclase MsGC-I is strongly expressed in higher order neuropils in the brain of *Manduca sexta*. *J. Exp. Biol.* **204**, 305-314.

Nishiyama, M., Hoshino, A., Tsai, L., Henley, J. R., Goshima, Y., Tessier-Lavigne, M., Poo, M. M. and Hong, K. (2003). Cyclic AMP/GMP-dependent modulation of Ca^{2+} channels sets the polarity of nerve growth-cone turning. *Nature* **424**, 990-995.

Oppliger, F. Y., Guerin, P. M. and Vlimant, M. (2000). Neurophysiological and behavioural evidence for an olfactory function for the dorsal organ and a gustatory one for the terminal organ in *Drosophila melanogaster* larvae. *J. Insect Physiol.* **46**, 135-144.

Sambrook, J., Fritsch, E. F. and Maniatis, T. (1989). *Molecular Cloning.* Cold Spring Harbor: Cold Spring Harbor Laboratory Press.

Schmidt, H., Werner, M., Heppenstall, P. A., Henning, M., More, M. I., Kuhbandner, S., Lewin, G. R., Hofmann, F., Feil, R. and Rathjen, F. G. (2002). cGMP-mediated signaling via cGKIalpha is required for the guidance and connectivity of sensory axons. *J. Cell Biol.* **159**, 489-498.

Shah, S. and Hyde, D. R. (1995). Two *Drosophila* genes that encode the alpha and beta subunits of the brain soluble guanylyl cyclase. *J. Biol. Chem.* **270**, 15368-15376.

Stocker, R. F. (1994). The organization of the chemosensory system in *Drosophila melanogaster*: a review. *Cell Tissue Res.* **275**, 3-26.

Sullivan, W., Ashburner, M. and Hawley, R. S. (2000). Drosophila *Protocols*. Cold Spring Harbor: Cold Spring Harbor Laboratory Press.

Younossi-Hartenstein, A. and Hartenstein, V. (1997). Pattern, time of birth, and morphogenesis of sensillum progenitors in *Drosophila*. *Microsc. Res. Tech.* **39**, 479-491.

Yu, S., Avery, L., Baude, E. and Garbers, D. L. (1997). Guanylyl cyclase expression in specific sensory neurons: a new family of chemosensory receptors. *Proc. Natl. Acad. Sci. USA* **94**, 3384-3387.

Zhao, Y., Schelvis, J. P. M., Babcocj, G. T. and Marletta, M. A. (1998). Identification of the histidine 105 in the β1 subunit of soluble guanylate cyclase as the heme proximal ligand. *Biochemistry* **37**, 4502-4509.